Applied Catalysis B: Environmental 176–177 (2015) 578–585

Contents lists available at ScienceDirect

Applied Catalysis B: Environmental

journal homepage: www.elsevier.com/locate/apcatb

Eco-efficient TiO_2 modification for air pollutants oxidation

S. Karapati [a], T. Giannakopoulou [a], N. Todorova [a], N. Boukos [a], D. Dimotikali [b], C. Trapalis [a,*]

[a] Institute of Nanoscience & Nanotechnology, NCSR Demokritos, Ag. Paraskevi, 15343 Athens, Greece
[b] National Technical University of Athens, Department of Chemical Engineering, 15780 Athens, Greece

ARTICLE INFO

Article history:
Received 17 January 2015
Received in revised form 30 March 2015
Accepted 6 April 2015
Available online 8 April 2015

Keywords:
Hydrophilicity
TiO_2
Modification
Photocatalysis
NO*x* removal

ABSTRACT

In the present work, the surface of P25 Evonik Degussa TiO_2 nanoparticles was modified with silane coupling agent 3-(2-aminoethylamino) propyltrimethoxy-silane (AAPTMS) at low temperature conditions to increase the hydrophilicity and De-NOx ability of the photocatalyst. The modified nanoparticles showed excellent stability in water. Their hydrodynamic diameter and polydisperse index were reduced in comparison with P25 and negatively charged surface was observed. The FTIR spectra revealed -NH_2 groups deformation which suggests interaction between surfactant's amino groups (–NH_2) with surface hydroxyl groups of TiO_2. The thermal analysis depicted combustion of the attached modifier in an elevated temperature range (300–800 °C). The AAPTMS-TiO_2 particles exhibited higher activity in NOx oxidation in comparison with the bare P25 and remarkable NO*x* removal ability that was attributed to the surface modification of the nanoparticles with hydrophilic AAPTMS groups.

1. Introduction

Nowadays, functional engineering materials with photocatalytic properties are of great importance for the industry and society. Environmental chemistry studies show that they participate in the removal of inorganic air pollutants (NO*x*), oxidative decomposition of volatile organic compounds (VOCs) and biological species (bacteria, viruses) [1,2] which have been accumulated into urban cities and downgrade to a serious extent the human life and environmental quality as well. Thus, the development of advanced materials with high photocatalytic effectiveness will contribute to the inhibition of serious health threats such as respiratory illnesses, lung cancer, emphysema and environmental issues such as acid rain and reduced vegetable growth [3,4].

Titanium dioxide, TiO_2, an *n*-type semiconductor, appears to be preferred photocatalyst among others due to its exceptional optical and electronic properties, suitable band gap energy for redox reactions, non toxicity to the human body and environment, inertness to chemical environment, long-term photostability, structural stability and low cost as well [5–8]. The preparation method and the properties of the photocatalyst influence to a great extent its photocatalytic activity. Thus, the synthesis of TiO_2 via hydrothermal treatment in presence of fluoride compound promote the formation of {0 0 1} TiO_2 facets exhibiting very high photocatalytic activity [9]. Also, it has been established that the decrease of particles size [10], the increased amount of surface hydroxyl groups [11] and defects [12,13] etc., positively affect catalytic effectiveness.

It has been clearly established that the hydrophilicity is an influential factor for the photocatalytic activity of the TiO_2. Under UV-irradiation, TiO_2 induces superhydrophilicity which allows water to spread over the surface rather than remaining as droplet [14], whilst in the dark the photocatalyst surface is gradually reverted to less hydrophilic [15]. Hydrophilic TiO_2 has found various technological applications such as anti-fogging, self-cleaning coatings in cars, glass windows as well as component of large building surfaces for decrease of harmful air pollutants concentration such as NOx, VOCs, etc. [16].

It is widely accepted that the degradation of inorganic and organic pollutants begins with the generation of electron-hole pairs [17] after TiO_2 photoexcitation with energy greater or equal to that of its band gap:

$$TiO_2 \xrightarrow{UV} h^+ + e^- \quad (1)$$

The excited electrons (e^-) are transferred to the conduction band leaving behind positive holes (h^+) in the valence band. These charge carriers recombine or react with oxygen molecules and hydroxyl anions respectively. Hydroxyl OH• and superoxide HO_2• radicals are produced through redox reactions utilizing the available from the environment H^+ ions as well:

$$OH^- + h^+ \rightarrow OH^\bullet \quad (2)$$

$$O_2 + e^- \rightarrow O_2^- \quad (3)$$

* Corresponding author. Tel.: +30 210 65 03 343; fax: +30 6973053974.
E-mail address: trapalis@ims.demokritos.gr (C. Trapalis).

http://dx.doi.org/10.1016/j.apcatb.2015.04.012
0926-3373/

The active $OH^{\bullet}$ species oxidize the NO gas adsorbed on TiO_2 surface to gaseous NO_2.• The final products of this procedure are nitrate ions (NO_3^-). The reaction mechanism is presented as follows [18–20]:

$$NO + 2OH^{\bullet} \rightarrow NO_2 + H_2O \quad (4)$$

$$2NO + {}^{\bullet}O_2^- \rightarrow 2NO_2 \quad (5)$$

$$NO_2 + OH^{\bullet} \rightarrow NO_3^- + H^+ \quad (6)$$

$$3NO_2 + 2OH^- \rightarrow 2NO_3^- + NO + H_2O \quad (7)$$

According to [20–21] the hydroxyl radicals seem to be the main responsible oxidants converting NO to NO_2 and NO_2 to NO_3^-. Thus, increase of OH groups improves the photocatalytic activity in multiple ways.

The improvement of the hydrophilic properties can be accelerated via the intensive presence of OH groups on TiO_2 surface [13]. These groups interact with the photogenerated holes (h^+) from TiO_2 surface resulting in formation of hydroxyl radicals ($OH^{\bullet}$) which are powerful active species responsible for the photocatalytic oxidation [22]. What is more, the enhancement of hydroxyl groups according to [23] contributes to intensive adsorbance of oxygen molecules which constitute trapping sites for the photogenerated electrons (e^-). Thus, the recombination of holes and electrons is inhibited and a greater amount of hydroxyl radicals are available for photocatalytic oxidation.

It is important to develop hydrophilic TiO_2 through scalable and low cost procedures. The modification in aqueous solutions is suggested due to lack of flammability, toxicity, low environmental risk and cost [24]. Low temperature procedures are also pursued in order to minimize energy consumption. In this respect, the use of colloidally stable and eco-friendly dispersions for TiO_2 functionalization can be considered for large industrial scale production of nanoparticles with desirable behavior and enhanced photacatalytic activity [16].

Silica sources have already been employed to modify TiO_2 nanoparticles for changing surface charge [25], decreasing nanoparticles aggregation [26], improving its mechanical and photocatalytic properties and dispersion stability in organic and aqueous media [27]. In addition, the TiO_2 nanoparticles have been endowed with the function of hydrophilicity via chemical treatment of TiO_2 surface with inorganic [14,28,29] and organic silane compounds [30,31]. Both increase [28] and decrease [29,32,33] of the photocatalytic activity after treatment have been reported.

According to reference [28] the modification of P25 nanoparticles with tetraethylorthosilicate (TEOS) on glazed ceramic tiles resulted in improved hydrophilicity and photocatalytic activity of TiO_2-particles under visible-light irradiation in degradation of RhB. This fact was attributed to the reduction of particle size and higher surface area of modified nanoparticles compared to bare TiO_2 since TEOS alone is not featured by photocatalytic oxidation properties. Contrariwise, in [29] it was reported that the improvement of hydrophilicity of the TiO_2–SiO_2 core shell structure was accompanied with reduction of photocatalytic activity in degradation of the organic dye methylene blue in water. The suppression of the photocatalytic activity was assigned to the low reducing power of the photogenerated electrons and the covering of the TiO_2 nanoparticles with inactive silica shells. The formation of Ti—O—Si bonding through condensation reactions between hydroxyl groups from TiO_2 surface and silanol groups from the silane compounds results in creation of coating around the TiO_2 nanoparticles which suppresses the photocatalytic activity of composite nanoparticles in comparison with bare TiO_2 [33].

Alkaline surfactant 3-(2-aminoethylamino) propyltrimethoxysilane (AAPTMS) with structural formula

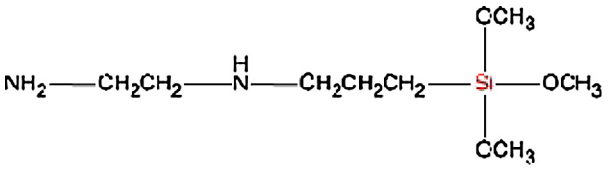

is frequently used as modifier of different oxides for a variety of purposes. Thus, AAPTMS coated magnetic nanoparticles were used for separation of inorganic arsenic from environmental water utilizing the affinity of the AAPTMS functional group –NH–CH_2–CH_2–NH_2 to As(V) [34]. Also, AAPTMS has been employed in synthesis of sorbent materials and specifically for functionalization of silica matrix in order to preconcentrate Cr(III) and Cr(VI) species, as well as to improve the hydrophilicity of nanocomposite coatings [35].

The present work deals with modification of commercial titania P25 with surfactant AAPTMS in water media. In these conditions, bonding between the surfactant molecule and the TiO_2 through the NH_2 part of the former is targeted, while additional hydrophilicity of the modified TiO_2 is expected due to hydrolysis of the silicon Si–$(OCH_3)_3$ part of the surfactant. The obtained modified photocatalysts were tested in NOx oxidation where improved activity is projected as a result of enhanced formation of $OH^{\bullet}$ radicals that are governing the De-NOx process.

2. Materials and methods

2.1. Materials and preparation of the samples

Commercial TiO_2 powder P25 (Evonic Degussa) was used. The silane coupling agent 3-(2-aminoethylamino) propyltrimethoxysilane ($C_8H_{22}N_2O_3Si$) was purchased from Sigma–Aldrich.

2 g of P25 nanoparticles were dispersed in 200 ml distilled H_2O using tip sonicator (Hielseher, UIP 100hd) functioning at 50% amplitude for 5 min (pH ~ 5). Different amounts of 3-(2-aminoethylamino) propyltrimethoxysilane ($C_8H_{22}N_2O_3Si$) were added to titania suspension (Table 1). The obtained emulsions with pH ~ 11 were kept under vigorous stirring at 50 °C for 18 h. The modified titania nanoparticles were collected by centrifugation (9000 rpm, 5 min), washed with acetone and ethanol consequently and dried at room temperature for 24 h.

2.2. Methods of characterization

Fourier Transform Infrared Spectroscopy (FT- IR) was used to investigate the presence of possible bonds between surfactant and titania nanoparticles. Instrument EQUINOX 55/S, BRUKER operating in Diffuse Reflectance mode was employed. The width of the energy band gap of the semiconductors was calculated employing the Kubelka–Munk function [36]. The samples consisted of 95 % KBr and 5% photocatalyst were scanned in wavenumber range 4000–400 cm^{-1}. The thermal behavior of modified nanoparticles was determined by Thermal Gravimetric Analysis using Perkin-Elmer Pyris TGA instrument. The samples were heated in a temperature range of 30–800 °C with a rate of 10 °C/min using air. Dynamic light scattering technique was employed to determine the particle hydrodynamic diameter and polydisperse index in water media. Zeta potential measurements using Zeta-sizer Nanoseries, Malvern instrument were carried out so as to estimate the surface charge of modified nanoparticles as a function of pH. Light absorption measurements in wavelength range 350–800 nm were performed using UV UV2100, Shimadzu spectrophotometer in order to estimate the energy band gap of the photocatalysts before and after modification. Morphological characterization of modified nanoparticles was conducted through transmission electron microscopy (TEM, Philips CM20) operated at 200 kV and equipped with the image filter GATAN GIF 200. EDX analyses were carried

Table 1
Samples nomination and the measured hydrodynamic diameter, polydisperse index, weight loss and Si content.

Samples	Molar ratio AAPTMS/P25	Average hydrodynamic diameter (nm)	Polydisperse index	Weight loss (%)	Si content (wt%)	Si content (at%)
P25	–	265.1	0.249	3.45	–	–
A3	0.3	234.2	0.284	7.24	2.63	4.41
A6	0.6	196.0	0.250	8.77	4.80	7.91
A9	0.9	158.3	0.120	6.65	11.22	17.72
A18	1.8	273.2	0.343	8.39	4.07	6.75

out using FEI Inspect microscope with tungsten filament operating at 25 kV to investigate the morphology of modified TiO_2 nanoparticles.

The photocatalytic activity of the initial P25 and modified titania powders was examined using ISO DIS 22,197/1:2007 standard method based on NO oxidation to NO_2(gas) and NO_3^-(solid). The installation used and the experimental conditions are described in details in references [37–40]. Briefly, the powder materials (~1 g) were pressed in holders with exposed surface 3.89 cm^2. The samples were placed in photocatalytic reactor with Quartz cover where model air flow with rate 3 L/min, NO concentration 1 ppm and relative humidity 50% was supplied. After a short dark period of ~10 min, the photocatalytic activity was determined under UV-A (main peak at 350 nm) irradiation with intensity 10 W/m^2 and the illumination period of time was 1 h. The concentrations of the NO and NO_2 gases in the gas phase above the photocatalysts were monitored. The De-NOx ability was evaluated by the decrease of the total NOx (NO and NO_2) concentration in the gas flow.

The photonic efficiency (ζ) of the photocatalytic materials was evaluated through the ratio of the number of oxidized gas molecules to the number of incident photons for the entire illumination period according to the equation:

$$\zeta = \frac{\int_{t_0}^{t_1} \mathrm{AX} \times 10^{-6} \mathrm{dt}}{q_{n,p} T} \left(\mathrm{mol/einstein}\right),$$

where A (expressed in mol/s) is the gas flow rate (gas flow rate 3 L/min employed in the experiment is equivalent to ~2.08×10^{-3} mol/s); X (taken in ppm) is either the difference between the reactor inlet (~1 ppm) and outlet concentrations of NO and NOx pollutants or directly the outlet concentration of NO_2 pollutant at different time moments; $q_{n,p}$ (taken in Einstein/s) is the photon flux incident on the whole sample surface S which is given by the equation $q_{n,p} = IS/NI_{ph}$ where I is the incident light intensity, I_{ph} is the photon energy at a given λ ($\lambda = 350 \times 10^{-9}$ m) and N is the Avogadro number; $T = t_1 - t_0$ is the illumination period, t_0 and t_1 are the time moments when UV light was switched on and off.

3. Results and discussion

3.1. Fourier transform infrared spectroscopy (FT-IR)

Fig. 1 depicts the FT-IR spectra of pristine and modified titania nanoparticles as well as of the modifier AAPTMS. As for the bare titania photocatalyst (sample P25), the peaks at ~1630 cm^{-1} are attributed to the bending H—O—H vibrations of adsorbed molecular water. The broad intense absorption in the range of 900–400 cm^{-1} is associated with the vibrations of the bonds Ti—O and Ti—O—Ti of TiO_2. There is an extensive absorption between 3200 and 3600 cm^{-1} related to stretching bonding vibration of hydroxyl groups attached to TiO_2 surface [28,29,41,42].

The spectrum of the AAPTMS surfactant is consisted of the absorption peaks of its characteristic functional groups. The vibrations observed in the wavenumber range 3350–3380 cm^{-1} and 3280–3320 cm^{-1} are attributed to stretches of primary amines (—NH_2) [43] and the vibrations at ~3185 cm^{-1} to stretches of secondary amines (—NH) [44]. N—H bending vibrations of primary

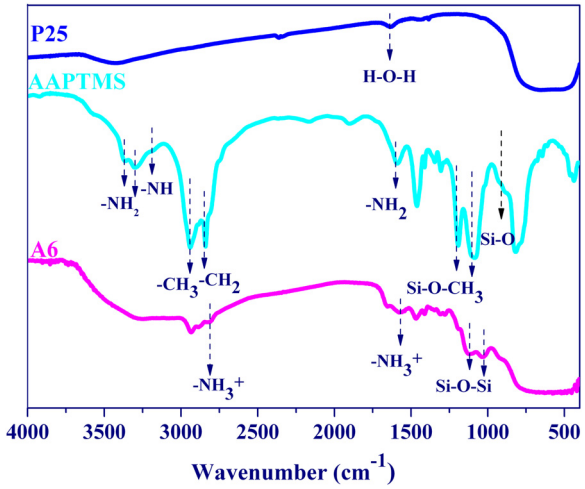

Fig. 1. FT-IR spectrum of neat P25 nanoparticles, AAPTMS surfactant and A6 modified TiO_2 nanoparticles.

amines (—NH_2) are also observed at around ~1600 cm^{-1} [32,33,43]. The absorption bands observed at ~2940 cm^{-1} and 2840 cm^{-1} correspond to stretching vibrations of —CH_3 and —CH_2 groups respectively, while the peak at ~1460 cm^{-1} is indicative for —CH_3 groups bending vibrations. The strong doublet at ~1194 cm^{-1} and 1080 cm^{-1} is related to asymmetric and symmetric stretching vibrations of Si—O—CH_3 groups [45]. Finally, the weak peak at ~920 cm^{-1} is attributed to non-bridging and free Si—O bonds [46,47].

In the spectrum of the modified titania nanoparticles (sample A6), the absorption in the range of 3000–3600 cm^{-1} attributed to hydroxyl radicals is enlarged in comparison to the sample P25 indicating their enhanced hydrophilicity. The peaks of the alkyl groups at ~2930, 2870 and 1460 cm^{-1} [31–33,46] have lower inten-

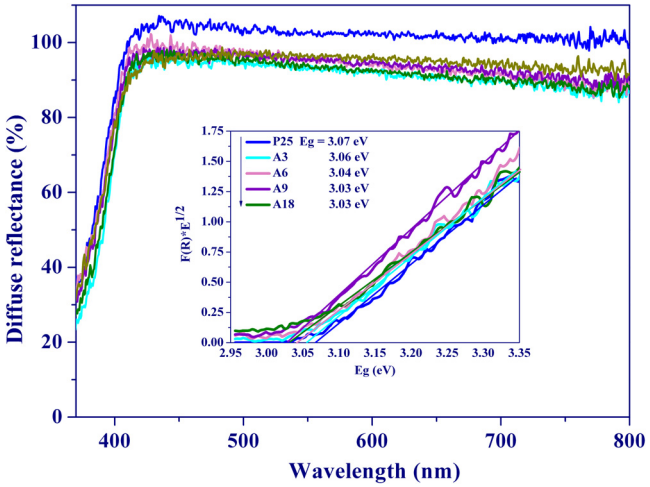

Fig. 2. Diffuse reflectance spectra of pure P25 and A3, A6, A9 A18 modified nanoparticles.

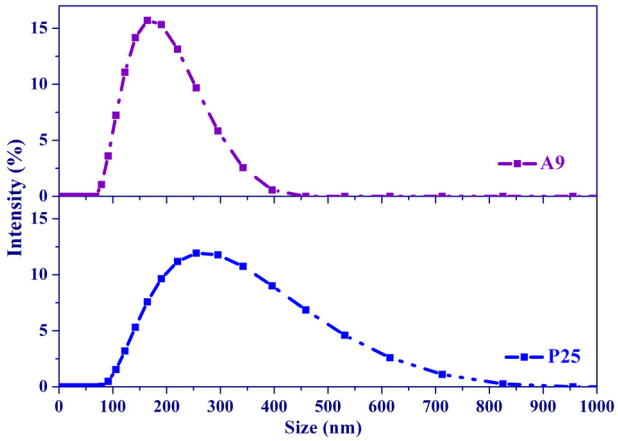

Fig. 3. Size distribution of pure P25 photocatalyst and A9 modified nanoparticles in water.

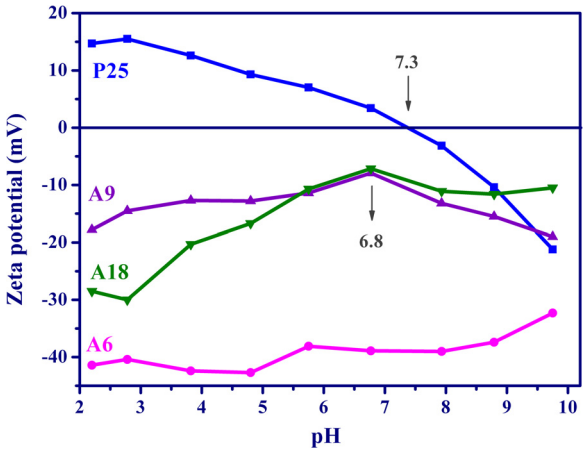

Fig. 4. Zeta potential – pH curves for pure P25 and A6, A9, A18 modified nanoparticles.

sity compared to those of AAPTMS indicating hydrolysis of the Si—(O—CH_3)$_3$ part of the modifier to Si–OH groups. The stretching vibrations of AAPTMS amine groups are absent or overlapped by hydroxyl absorption in the spectrum of the sample A6 and a new asymmetric vibration is observed at ~2800 cm^{-1}. Furthermore, bending vibrations of NH_2 groups at ~1600 cm^{-1} were shifted to lower wavenumbers (~1570 cm^{-1}). The peak at ~2800 cm^{-1} can be assigned to stretching while those at ~1570 cm^{-1} to asymmetric bending vibrations of NH_3^+ resulting from the electrostatic interaction or hydrogen bonding between —NH_2 groups and hydroxyl groups on TiO_2 surface [33,43,48–52]. The new peaks observed at ~1120 cm^{-1} could be assigned to asymmetric stretching vibration of Si—O—Si bonding or C—N bond. The new band at ~1032 cm^{-1} corresponds to Si—O—Si formed by condensation reactions of silanol groups during modification [51]. The peak at 920 cm^{-1} assigned to free Si—O bonds of the surfactant can also be observed in the spectrum of the modified sample A6. Thus, the shift of the —NH_2 groups and the preservation of the Si—O groups suggest that, during the modification, the TiO_2 interacts with the AAPTMS surfactant mainly through its amine part but not through its Si—OH part.

3.2. Light absorption measurements

Fig. 2 shows the diffuse reflection (DR) spectra of the bare TiO_2 and AAPTMS-modified nanoparticles. In all modified photocatalysts, increased absorption in the region between 800 and 450 nm was observed. Also a slight shift of the main absorption to visible light (~400 nm) wavelengths was recorded which reflects the lower values for the width of the effective band gap (inset of Fig. 3) found for the modified titania in comparison with the initial P25. The A9 and A18 photocatalysts exhibited the lowest band gap energy (3.03 eV) implying that the semiconductor structure is differentiated by the presence of electron states near the bottom of the conduction band and the top of the valence band [53]. Thus, the surface modification of TiO_2 nanoparticles could be considered to some extent as surface doping and effectiveness under visible light irradiation could be expected.

3.3. Dynamic light scattering measurements (DLS)

The size distribution of unmodified P25 and AAPTMS-modified nanoparticles was obtained by Dynamic Light Scattering technique using water as dispersion medium. The concentration of the unmodified and modified photocatalysts was chosen to be 5 mg/L to avoid instability and formation of agglomerates.

The modified by the hydrophilic surfactant nanoparticles exhibited better dispersion stability in the water compared to the neat photocatalyst. From Table 1 it can be perceived that the average size and polydisperse index diminished with the increase of the surfactant concentration in comparison to P25. The lowest average size and polydisperse index were recorded for sample A9. The size distribution curves of this sample and non-modified P25 are depicted in Fig. 3. It is obvious that the size range of A9 agglomerates (100–500 nm) decreases compared to the size range of the P25 agglomerates (100–800 nm). Similar to A9 results are observed for the rest of modified nanoparticles (samples A3 and A6), while the sample A18 exhibited enhanced agglomeration in comparison to P25 and the rest of modified powders. This outcome is attributed to excess of surfactant which due to the high concentration remains unreacted.

3.4. Zeta potential measurements

The results from zeta potential measurements for pure P25 and modified nanoparticles are presented in Fig. 4. The zeta potential values of non-modified TiO_2 vary from +15 to −23 mV and the isoelectric point was measured at pH ~7.3–7.4. It can be observed that after modification with AAPTMS surfactant the surface character of nanoparticles changed drastically. Specifically, only negative surface charge of −45 to −10 mV was recorded over the measured pH range. The increase of the negative surface charge enhances the electrostatic repulsive forces between electrical double layer around the nanoparticles and the aqueous medium which override attractive Van Der Waals forces between the nanoparticles. Thus, the agglomeration of the nanoparticles is suppressed and the hydrodynamic diameter is reduced [54]. The sample A6 exhibited the strongest negative charge and isoelectric point for this sample was not observed. Although a clear isoelectric point can not be seen for the samples A9 and A18, it could be assumed that the isoelectric point of these samples is positioned around the pH 6.8 since the Z-potential curves exhibit maximum at this pH and the measured Z-potential values are close to 0.

It could be speculated that if in our experiment the silanol groups of the modifier had interacted with the TiO_2 surface to form Ti—O—Si bonds, then the unreacted –NH_2 groups would shift the isoelectric point of modified nanoparticles to values close to 10 due to their alkaline character [31,32]. However, in our results the isoelectric point of AAPTMS–modified nanoparticles decreased in comparison to the non-modified TiO_2, indicating that the amine groups have interacted with TiO_2.

The alkaline character of the AAPTMS surfactant results in increase of the OH groups concentration around the TiO_2 particle and in protonation of the amine groups of the surfactant. Hence, hydrogen or ionic bonding between the negatively charged OH^- groups and positively charged NH_3^+ is promoted [33,49,55,56].The $Si—(O—CH_3)_3$ part of the AAPTMS surfactant is hydrolyzed to form trisilanols ($Si(OH)_3$) [49]. This procedure is accelerated due to the presence of the surfactant's amine group. The imperative presence of water inhibits to a great extent the condensation reaction of silanol groups to siloxane (Si—O—Si) bonding [50]. As a result, a coating of —SiOH groups is formed around the TiO_2 nanoparticles the OH groups of which are responsible for the negative charge of the modified nanoparticles (Fig. 5). This outcome is in accordance with the DLS results concerning the enhanced hydrophilicity and photocatalytic activity in air pollutants oxidation is expected.

3.5. Thermal analysis

Fig. 6 depicts the weight loss (TG) and DTG curves of P25 and AAPTMS modified photocatalysts. From the Fig. 6 and Table 1 it is evident that the P25 is thermally stable with weight loss of

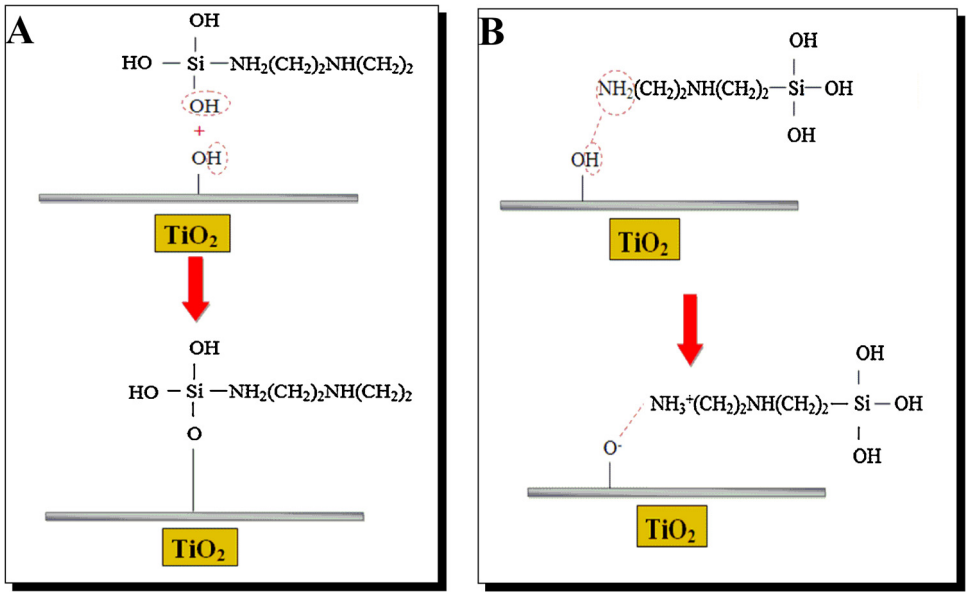

Fig. 5. Functionalization mechanisms suggesting grafting of hydrolyzed AAPTMS to TiO_2 surface through its: (a) silicon and (b) amino groups.

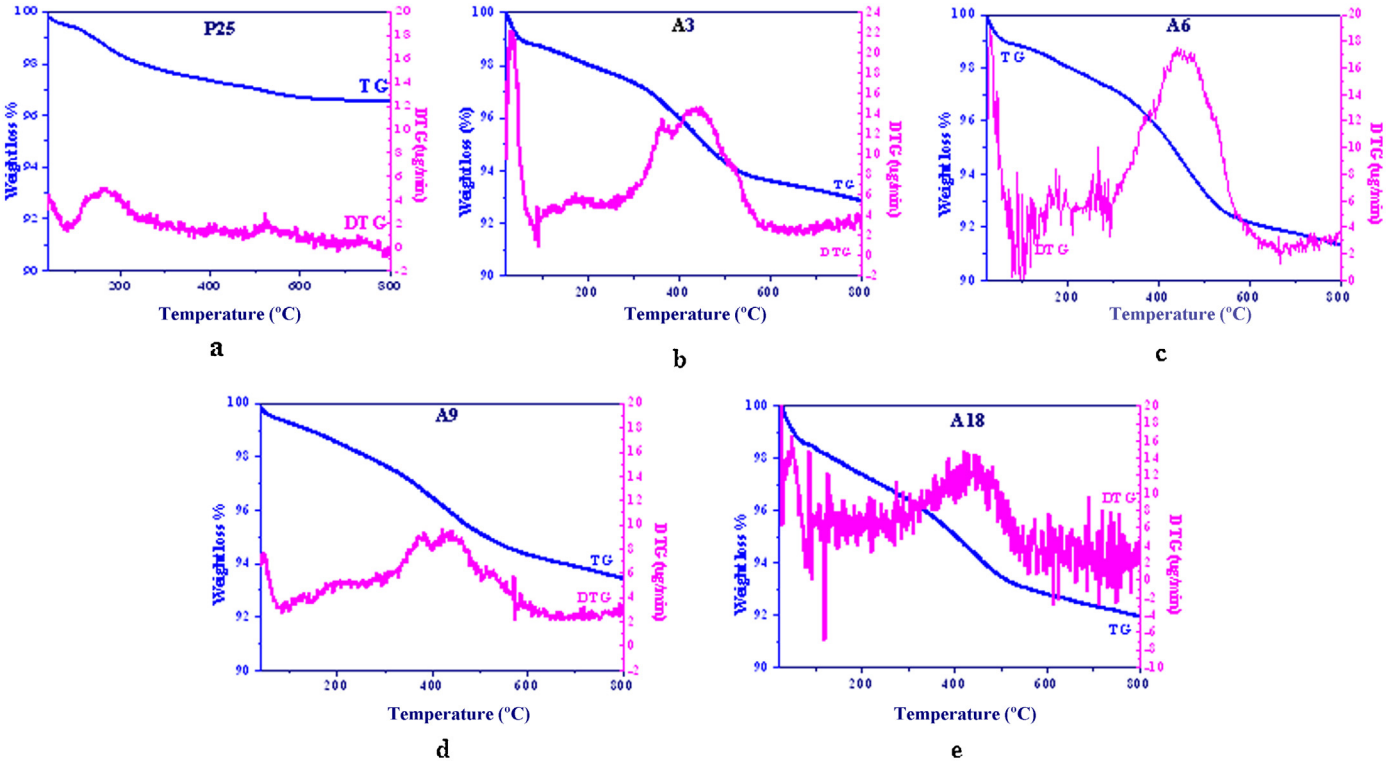

Fig. 6. TG/DTG curves of pure P25 and modified A3, A6, A9, A18 photocatalysts.

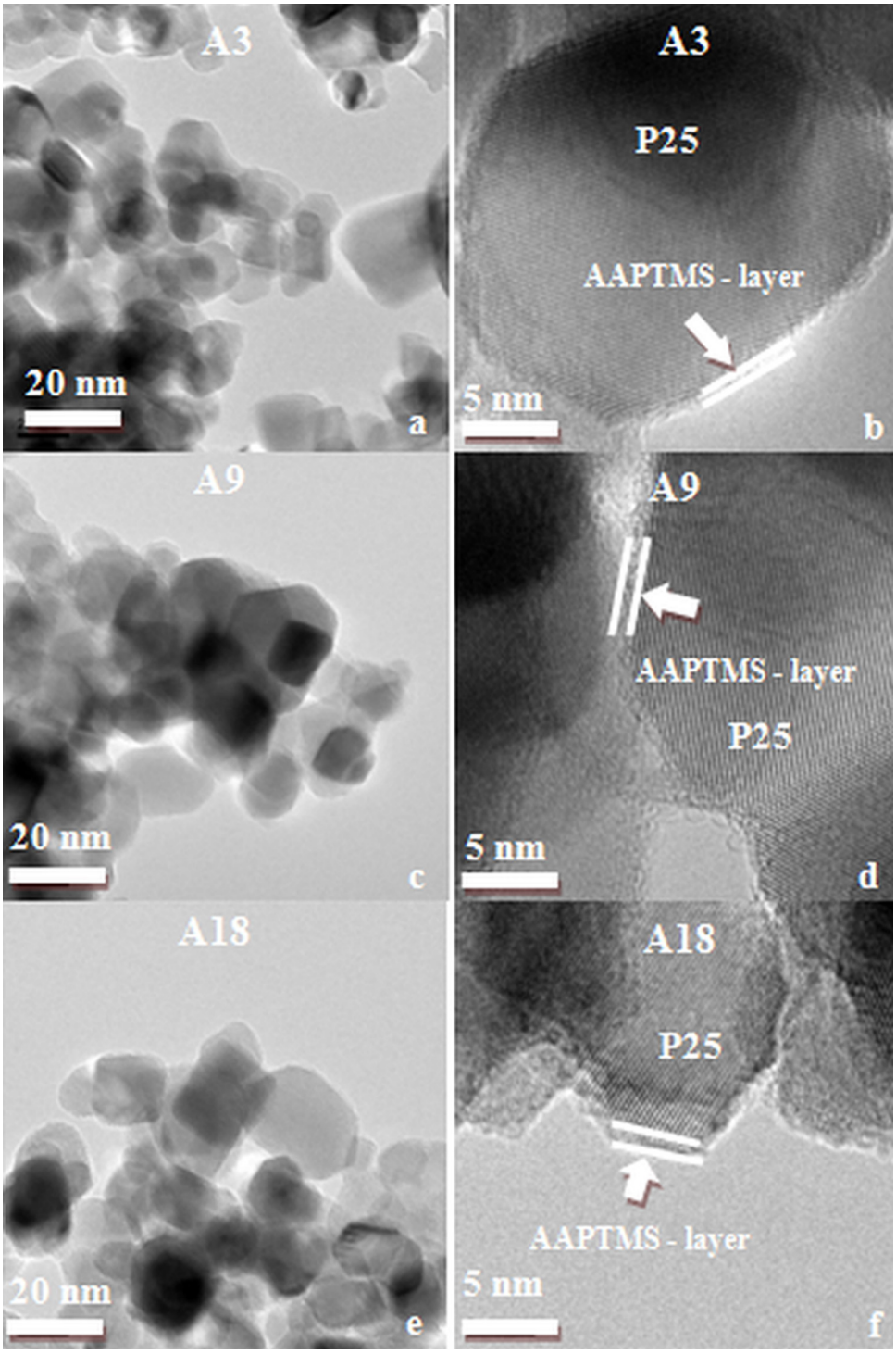

Fig. 7. High Resolution TEM micrographs of A3, A9, A18.

only 3.45% for the entire temperature range. The rest of modified nanoparticles presented enhanced weight losses with the highest weight loss 8.77% to be observed for the sample A6. With the increase of the surfactant concentration (A9 and A18) the weight loss slightly decreased suggesting reduced amount of AAPTMS attached to the TiO_2 particles.

For the modified nanoparticles, several weight losses were recorded which took place in different temperature ranges. The first weight loss occurred from 30 to 100 °C and it is assigned to water evaporation phenomena. The second loss observed between ~100 and ~350 °C is attributed to the volatilization of organic compounds attached to titania nanoparticles via weak hydrogen bounding [31,32,43].

The third weight loss is depicted from 350 to 500 °C. In this temperature range AAPTMS layer arranged to TiO_2 surface is combusted [49]. Probably, in this case AAPTS molecules are stronger grafted to TiO_2 surface through electrostatic interaction such as ionic bonding.

In this temperature range, the dehydration of silanols (SiOH) occurred as well as combustion of nitrogeneous species.

Table 2
Photonic efficiency (ζ) of the pure and modified P25 powders under UV light illumination for NO oxidation, NO_2 formation and NO_x removal.

Sample		P25	A3	A6	A9	A18
ζ (mol/einstein)	ζ_{NO}	0.01200	0.02312	0.05097	0.04520	0.02956
	ζ_{NO2}	0.00736	0.00192	0.01436	0.01042	0.00743
	ζ_{NOx}	0.00460	0.02120	0.03660	0.03478	0.02213

Specifically, the peak of DTG curve (samples A6 and A9) centered at 380 °C is related to the combustion of amino- species while the peak centered around 500 °C (samples A3, A6, A9, A18) is assigned to dehydration of silanols [51,56]. The latter is more prominent in case of sample A6 indicating a strong dehydration process while for the samples A9 and A18 the peak is less intensive. These results are in good agreement with Zeta Potential measurements showing less negative charge in case of samples A9 and A18.

Finally, the weak weight loss between 550 and 800 °C is ascribed to the complete removal of AAPTMS surfactant attached to TiO_2 nanoparticles [56,57].

3.6. Transmission electron microscopy (TEM)

Fig. 7 shows TEM high resolution micrographs of the A3, A9 and A18 modified nanoparticles. For the modified sample A3, an amorphous Angstrom scaled coating covering the majority of TiO_2 nanocrystals can be observed. As the molar ratio surfactant/TiO_2 increased, more TiO_2 nanoparticles were covered with AAPTMS layer and the thickness of which was slightly increased. These findings are in good agreement with the results from Thermal Analysis and SEM/EDX (Table 1) showing that the aminosilane coverage of the TiO_2 particles enhances with the increase of the surfactant concentration.

3.7. Photocatalytic De – NO_x ability

The photocatalytic activity of the powder photocatalysts was evaluated as for NO air pollutant oxidation. It should be mentioned that all the materials did not exhibit catalytic activity in absence of light. The photonic efficiencies of the P25 and the AAPTMS-capped photocalysts are comparatively presented in Fig. 8 and Table 2. It can be perceived that the modification of P25 with hydrophilic AAPTMS surfactant resulted in improved photocatalytic activity as for NO oxidation and NOx removal as well. Specifically, for all the modified samples the NO degradation was enhanced 2–5 times in comparison with P25, while the NOx removal was improved even more. The best photonic efficiencies were depicted for A6 modified powder, i.e., 5 times in NO oxidation and 9 times in NOx removal. For the samples with higher surfactant concentrations (A9, A18) the photonic efficiency, although higher than P25, is lower than sample A6. This outcome can be connected to the excess of surfactant during the modification leading to less efficient hydrolysis of its propylmethoxysilane groups, which react with SiOH, cover the TiO_2 surface and deteriorates the photocatalytic activity.

The remarkable De-NOx activity of AAPTMS-modified nanoparticles can be attributed to the reduced average size leading to their increased hydrophilicity as recorded by the DLS analysis. In addition, the enhanced negative charge of the treated nanoparticles revealed by the Zeta potential results, suggests that a greater amount of hydroxyl groups can be found around modified TiO_2 surface. Thus, more reactive $OH^{\bullet}$ species crucial for the De-NOx process, can be produced and involved in the NO oxidation reactions.

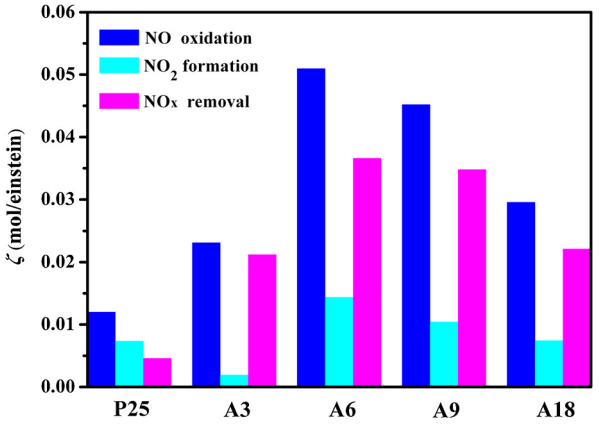

Fig. 8. Photonic efficiency (ζ) of pure P25 and modified A3, A6, A9, A18 photocatalysts.

4. Conclusions

Surface-functionalized TiO_2 nanoparticles were prepared through treatment with AAPTMS surfactant in aqueous medium. FT-IR demonstrated that during the modification, the TiO_2 interacts with the AAPTMS surfactant mainly through its amine NH_2 part but not through its Si—OH part. The AAPTMS-grafting on photocatalyst's surface was verified by Thermal Analysis. Amorphous coating originating from the surfactant was observed around the titania nanoparticles. Also, lower aggregation, increased hydrophilicity and negative charge were observed for the modified nanoparticles compared to P25.

Finally, the modified titania powders exhibited excellent photocatalytic activity under UV irradiation in NO oxidation and NOx removal. Their superior photonic efficiency was related to the functionalization mechanism and the improved hydrophilicity.

The applied modification route could be utilized for large scale, eco-friendly, cost-effective production of TiO_2 nanoparticles with high De-NOx ability.

Acknowledgements

This work was partially supported by the General Secretariat for Research and Technology of Greece under the projects 09SYN-42-925 ARISTON, 12SLO ET30 1162 and 12CHN205 PhotoTiGRA.

References

[1] S.H. Nam, S.J. Cho, C.K. Jung, J.H. Boo, J. Šícha, D. Heřman, J. Musil, J. Vlček, Thin Solid Films 519 (2011) 6944–6950.
[2] B. Tryba, M. Piszch, A.W. Morawski, Open Mater. Sci. J. 4 (2010) 5–8.
[3] S. Baidar, R. Volkamer, R. Alvarez, A. Brewer, F. Davies, A. Langford, H. Oetjen, G. Pearson, C. Senff, R. Michael Hardesty, Br. J. Environ. Clim. Change 3 (2013) 566–586.
[4] S.M. Al-Salem, A.R. Khan, Braz. J. Chem. Eng. 25 (2008) 683–696.
[5] B.X. Wei, L. Zhao, T.J. Wang, H. GaO, H.X. Wu, Y. Jin, Adv. Powder Technol. 24 (2013) 708–713.
[6] A.O. Ibhadon, P. Fitzpatrick, Catalysts 3 (2013) 189–218.
[7] F. Sayilkan, M. Asilturk, H. Sayilkan, Y. Onal, M. Akarsu, E. Arpac, Turk. J. Chem. 29 (2005) 697–706.
[8] S. Kimiagar, A. Nahal, M.R. Mohammadizadeh, T.G. Elahi, Phys. Scr. 88 (2013) 1–7.
[9] J. Yu, J. Low, W. Xiao, P. Zhou, M. Jaroniec, J. Am. Chem. Soc. 136 (2014) 8839–8842.
[10] H. Lin, C.P. Huang, W. Li, C. Ni, S. Ismat Shah, Y.-H. Tseng, Appl. Catal. B: Environ. 68 (2006) 1–11.

[11] J. Wang, X. Liu, R. Li, P. Qiao, L. Xiao, J. Fan, Catal. Commun. 19 (2012) 96–99.
[12] X. Zhang, J. Qin, Y. Xue, P. Yu, B. Zhang, L. Wang, R. Liu, Sci. Rep. 4 (2014) 4596.
[13] M.E. Simonsen, Z.S. Li, E.G. Sogaard, Appl. Sur. Sci. 255 (2009) 8054–8062.
[14] K. Guan, Surf. Coat. Tech. 191 (2005) 155–160.
[15] A. Kolouch, M. Horáková, P. Hájková, E. Heyduková, P. Exnar, P. Spatenka, Plasma Phys. 12 (2006) 198–200.
[16] B. Faure, G. Salazar-Alvarez, A. Ahniyaz, I. Villaluenga, G. Berriozabal, Y.R. De Miguel, L. Bergstrom, Sci. Technol. Adv. Mater. 14 (2013) 023001.
[17] M. Horprathuma, P. Eiamchai, P. Limnonthakul, N. Nuntawonga, P. Chindaudoma, A. Pokaipisit, P. Limsuwan, J. Alloys Compd. 509 (2011) 4524–4540.
[18] G. Husken, M. Hunger, H.J.H. Brouwers, Build. Environ. 44 (2009) 2463–2474.
[19] J.S. Dalton, P.A. Janes, N.G. Jones, J.A. Nicholson, K.R. Hallam, G.C. Allen, Environ. Pollut. 120 (2002) 415–422.
[20] K. Hashimoto, K. Wasada, N. Toukai, H. Kominami, Y. Kera, J. Photochem. Photobiol. A 136 (2000) 103–109.
[21] M.M. Ballari, M. Hunger, G. Husken, H.J.H. Brouwers, Appl. Catal. B Environ. 95 (2010) 245–254.
[22] H.S. Jung, J.K. Lee, M. Nastasi, J.R. Kim, S.W. Lee, J.Y. Kim, J.S. Park, K.S. Hong, H. Shin, Appl. Phys. Lett. 88 (2006) 013107.
[23] J. Yu, H. Yu, B. Cheng, M. Zhou, X. Zhao, J. Mol. Catal. A: Chem. 253 (2006) 112–118.
[24] J. Chen, S.K. Spear, J.G. Huddleston, R.D. Rogers, Green Chem. 7 (2005) 64–82.
[25] H. Park, Y. Park, W. Kim, W. Choi, J. Photochem. Photobiol. C: Photochem. Rev. 15 (2013) 1–20.
[26] R. Tomovska, V. Daniloska, J.M. Asua, Appl. Surf. Sci. 264 (2013) 670–673.
[27] X.W. Li, R.G. Song, Y. Jiang, C. Wang, D. Jiang, Appl. Surf. Sci. 276 (2013) 761–768.
[28] P. Zhang, J. Tian, R. Xu, G. Ma, Appl. Surf. Sci. 266 (2013) 141–147.
[29] H.S. Lee, S.M. Koo, J.W. Yoo, J. Ceram. Process. Res. 13 (2012) 300–303.
[30] N.R. Jana, C. Earhart, J.Y. Ying, Chem. Mater. 19 (2007) 5074–5082.
[31] A. Ershad-Langroudi, S. Gharazi, A. Rahimi, D. Ghasemi, Appl. Surf. Sci. 255 (2009) 5746–5754.
[32] J. Zhao, M. Milanova, M.M.C.G. Warmoeskerken, V. Dutschk, Colloid Surf A: Physicochem. Eng. Aspects 413 (2012) 273–279.
[33] E. Ukaji, T. Furusava, M. Sato, N. Suzuki, Appl. Surf. Sci. 254 (2007) 556–563.
[34] C. Huang, W. Hie, X. Li, J. Zhang, Microchim. Acta 173 (2011) 165–172.
[35] C.R.T. Tarley, G.F. Lima, D.R. Nascimento, A.R.S. Assis, E.S. Ribeiro, K.M. Diniz, M.A. Bezerra, M.G. Segatelli, Talanta 100 (2012) 71–79.
[36] E.L. Simmons, Opt. Acta 19 (1972) 845–851.
[37] S. Karapati, T. Giannakopoulou, N. Todorova, N. Boukos, S. Antioxos, D. Papageorgiou, E. Chaniotakis, D. Dimotikali, C. Trapalis, Appl. Surf. Sci. 319 (2014) 29–36.
[38] N. Todorova, T. Giannakopoulou, S. Karapati, D. Petridis, T. Vaimakis, C. Trapalis, Appl. Surf. Sci. 319 (2014) 113–120.
[39] A. Mitsionis, T. Vaimakis, C. Trapalis, N. Todorova, D. Bahnemann, R. Dillert, Appl. Catal. B: Environ. 106 (2011) 398–404.
[40] T. Giannakopoulou, N. Todorova, G. Romanos, T. Vaimakis, R. Dillert, D. Bahnemann, C. Trapalis, Mater. Sci. Eng. B 117 (2012) 1046–1052.
[41] K. Balachandaran, R. Venckatesh, R. Sivaraj, Int. J. Eng. Sci. Technol. 2 (2010) 3670–3695.
[42] M. Burgos, M. Langlet, J. Sol–Gel Sci. Technol. 16 (1999) 267–276.
[43] P. Yuan, P.D. Saouthon, Z. Liu, M. Green, J. Hook, S. Antil, C. Kepert, J. Phys. Chem. C 112 (2008) 15742–15751.
[44] W.B. Mefteh, H. Touzi, Y. Chevalier, H.B. Ouada, A. Othmane, R. Kalfat, N. Jaffrezic-Renault, Sens. Actuators B 204 (2014) 723–733.
[45] T. Eren, J. Appl. Polym. Sci. 105 (2007) 1426–1436.
[46] H.K. Park, T.H. Ha, K. Kim, Langmuir 20 (2004) 4851–4858.
[47] F. Rubio, J. Rubio, J.L. Oteo, Spectrosc. Lett. 31 (1998) 199–219.
[48] B. Ingham, S.V. Chong, J.L. Tallon, J. Phys. Chem. B 109 (2005) 4936–4940.
[49] D. Zeroka, J.O. Jensen, J. Mol. Struct. 425 (1998) 181–192.
[50] K.C. Vrancken, K. Possemiers, P. Van Der Voort, E.F. Vansant, Colloids Surf. A: Phys. Chem. Eng. Asp. 98 (1995) 235–241.
[51] S. Yang, P. Yuan, H. He, Z. Qin, Q. Zhou, J. Zhu, D. Liu, Appl. Clay Sci. 62–63 (2012) 8–14.
[52] M. Raza, A. Bachinger, N. Zahn, G. Kickelbick, Materials 7 (2014) 2891–2895.
[53] D.Q. Fang, A.L. Rosa, Th. Frauenheim, R.Q. Zhangn, Appl. Phys. Lett. 94 (2009) 73116.
[54] K. Suttiponparnit, J. Jiang, M. Sahu, S. Suvachittanont, T. Charinpanitkul, P. Biswas, Nanoscale Res. Lett. 6 (2010) 1–8.
[55] B. Sceibe, E. Borowiak-Palen, R.J. Kalenczuk, Acta Phys. Pol. A 116 (2009) S150–S153.
[56] J. Wang, J. Sun, F. Wang, B. Ren, Appl. Surf. Sci. 274 (2013) 314–320.
[57] M. Sabzi, S.M. Mirabedini, J. Zohuriaan-Mehr, M. Atai, Prog. Org. Coat. 65 (2009) 222–228.